Environmental Modelling & Software 102 (2018) 138–154

Contents lists available at ScienceDirect

Environmental Modelling & Software

journal homepage: www.elsevier.com/locate/envsoft

Modelling marine trophic transfer of radiocarbon (^{14}C) from a nuclear facility

Kieran M. Tierney [a, b, *], Johanna J. Heymans [b], Graham K.P. Muir [a, b], Gordon T. Cook [a], Joe Buszowski [c], Jeroen Steenbeek [c], William J. Walters [d], Villy Christensen [c, e], Gillian MacKinnon [a], John A. Howe [b], Sheng Xu [a]

[a] Scottish Universities Environmental Research Centre, Rankine Avenue, Scottish Enterprise Technology Park, East Kilbride, G75 0QF, Scotland, UK
[b] The Scottish Association for Marine Science, Scottish Marine Institute, Oban, PA37 1QA, Scotland, UK
[c] Ecopath International Initiative Research Association, Barcelona, Spain
[d] Department of Mechanical and Nuclear Engineering, Pennsylvania State University, University Park, PA, 16802, USA
[e] Institute for the Oceans and Fisheries, University of British Columbia, Main Mall 2202, V6T1Z4, Vancouver, Canada

ARTICLE INFO

Article history:
Received 2 June 2017
Received in revised form
12 January 2018
Accepted 13 January 2018

Keywords:
Radiocarbon (^{14}C)
Radioactive discharges
Sellafield
Ecosystem model
Ecopath with ecosim
Ecotracer

ABSTRACT

Sellafield marine discharges of ^{14}C are the largest contributor to the global collective dose from the nuclear fuel industry. As such, it is important to understand the fate of these discharges beyond the limitations and scope of empirical analytical investigations for this highly mobile radioactive contaminant. Ecopath with Ecosim (EwE) is widely used to model anthropogenic impacts on ecosystems, such as fishing, although very few EwE studies have modelled the fate of bioavailable contaminants. This work presents, for the first time, a spatial-temporal ^{14}C model utilising recent developments in EwE software to predict the ecological fate of anthropogenic ^{14}C in the marine environment. The model predicted observed trends in ^{14}C activities between different species and through time. It also provided evidence for the integration of Sellafield ^{14}C in species at higher trophic levels through time.

Software availability

Name of software: Ecopath with Ecosim
Developer: Ecopath Research and Development Consortium
Contact address: Ecopath International Initiative Research Association, Barcelona, Spain
Contact email: ewedevteam@gmail.com
Year first available: 1991
Hardware required: PC
Software required: Windows XP service pack 3 or newer, Microsoft.NET Framework 4 Full Profile
Availability: Public, Open Source (GPLv2), freely available from www.ecopath.org (version used in this study available from developer)
Program language: Visual Basic.NET, C# Program size: 16 MB (basic installation)

1. Introduction

Understanding the ecological fate of anthropogenic radionuclides is necessary to determine any potentially hazardous consequences to the environment and to human populations. Although empirical studies are essential, they are often time-consuming, costly and impractical to conduct, particularly if basic information is required quickly (e.g. after accidental releases of radioactive material) or, if radioactive contamination is spread over a large area. Computer modelling provides an additional tool which can be both time- and cost-effective. The ecosystem modelling software suite, Ecopath with Ecosim (EwE) (Christensen and Walters, 2004), has undergone recent developments that aid its ability to model the ecological fate of environmental contaminants spatially. EwE has previously been used to model non-radioactive contaminants such as methyl-mercury in the Faroe Islands marine ecosystem (Booth

* Corresponding author. Scottish Universities Environmental Research Centre, Rankine Avenue, Scottish Enterprise Technology Park, East Kilbride, G75 0QF, Scotland, UK.
E-mail address: kieran.tierney@strath.ac.uk (K.M. Tierney).

https://doi.org/10.1016/j.envsoft.2018.01.013

and Zeller, 2005), chemical warfare agents in the Baltic Sea (Niiranen et al., 2008; Sanderson et al., 2010), polycyclic aromatic hydrocarbons (PAHs) in the Arctic (Larsen et al., 2016) and polychlorinated biphenyls (PCB) and mercury in the Great Lakes (McGill et al., 2017). EwE has also been used to model radioactive contaminants, including a hypothetical release of radiocarbon (^{14}C) in the Baltic Sea (Sandberg et al., 2007) and radiocaesium (^{137}Cs) in a simple, coastal marine ecosystem model for Fukushima (Walters and Christensen, 2017). Many of these studies considered temporal change in contaminant activity but not spatial variation. The EwE approach is appealing for modelling bioavailable contaminants, due primarily to its ease of use. There are over 400 unique EwE models published, making it the most extensively applied tool for modelling marine and aquatic ecosystems (Colleter et al., 2015). The extensive coverage of published EwE models also means that models may already exist for a specific ecosystem in which an environmental contaminant is present, or subject to a recent contamination event, and can be adapted for this purpose.

There are four components to EwE: 1) Ecopath, which describes a static, mass-balanced ecosystem (Polovina, 1984); 2) Ecosim, a time dynamic simulation module allowing for temporal changes and impacts to an ecosystem to be investigated (Walters et al., 1997); 3) Ecospace, where ecosystem changes can be explored both spatially and temporally (Walters et al., 1999); and 4) Ecotracer, which traces contaminants through the ecosystem (Walters and Christensen, 2017). While Ecosim/Ecospace solve biomass dynamic equations, Ecotracer simultaneously models contaminant flow and/or accumulation to the biological groups and environment as described in the base Ecopath model. Ecotracer and the equations it utilises are fully described in Walters and Christensen (2017). The development of the spatial-temporal EwE framework (Steenbeek et al., 2013) allows physical changes to occur in the Ecospace environment through time. As environmental contamination is typically non-ubiquitous and non-static, this is an appropriate development to consider for contaminant models where contaminant concentrations in the environment are both temporally and spatially variable.

In recent decades, several studies have accumulated a large body of data regarding the fate of ^{14}C discharged by the Sellafield nuclear fuel reprocessing facility in Cumbria, UK, to the marine environment (Begg et al., 1992, Cook et al., 1995, 1998, 2004; Gulliver et al., 2001, 2004; MacKenzie et al., 2004, Muir et al., 2015, 2017; Tierney et al., 2016, 2017a, 2017b). The most recent work has focussed on detailing the ecosystem uptake of ^{14}C in the Irish Sea (Muir et al., 2017), and the West of Scotland (Tierney et al., 2017a) marine environments, and has established a time-series of ^{14}C activities in marine mammals along the UK coastline (Tierney et al., 2017b). Sellafield discharges ^{14}C as low-activity waste effluent via pipelines to the Irish Sea in the dissolved inorganic phase, which is rapidly incorporated into the marine dissolved inorganic carbon (DIC) pool (Begg et al., 1992; Cook et al., 1995). In this manner, Sellafield ^{14}C spreads throughout the Irish Sea and is largely dispersed northward through the North Channel to the West of Scotland marine environment by prevailing currents (Gulliver et al., 2001). Whilst contemporary environmental releases of ^{14}C from Sellafield do not pose any direct radiological risk to critical consumer groups near Sellafield (Muir et al., 2017), releases of ^{14}C are still highly significant. ^{14}C has a long half-life (5730 years), is environmentally mobile, highly bioavailable and marine discharges are the largest contributor to the UK, European and global collective dose from Sellafield (Nuclear Decommissioning Authority, 2016).

The aim of this study was to construct an EwE contaminant tracing model for Sellafield ^{14}C in the UK marine environment, the 'Sellafield model', and to test it, primarily, using recent data compiled in Muir et al. (2017) and Tierney et al. (2017a, 2017b). This is the first time an EwE model has been tested on its ability to accurately predict the spatial ecosystem uptake and fate of radionuclides discharged routinely to the marine environment. The unique biogeochemical properties of ^{14}C, in being identical in its behaviour to stable carbon on an ecosystem level, coupled with its long half-life, make it an 'ideal' contaminant with which to evaluate the performance and applicability of the EwE model and Ecotracer utility for radioactive contamination scenarios.

2. Methods

2.1. Ecopath input

In EwE, functional groups are either specific species or a group of species deemed to have sufficiently similar functionality for the purposes of the model (Heymans et al., 2016). Functional groups require a number of input parameters to satisfy the Ecopath mass balance equation where consumption (C) = production (P) + respiration (R) + unassimilated food (U). The productivity of each functional group is defined in Ecopath by the equation:

$$P_i = Y_i + B_i.M2_i + E_i + BA_i + P_i.(1 - EE_i)$$

where for group i : P_i is the total production rate, Y_i is the total fishery catch rate, B_i is the biomass, $M2_i$ is the total predation rate, E_i is the net migration rate (emigration−immigration), BA_i is the biomass accumulation rate and EE is the ecotrophic efficiency of the group (Christensen and Walters, 2004). Ecotrophic efficiency is the proportion of a group's production that is explained in the model and this cannot exceed 1. Typical inputs to Ecopath include values for biomass (B), annual production/biomass (P/B) and either annual consumption/biomass (Q/B) or production/consumption (P/Q).

As Sellafield discharges ^{14}C into the Irish Sea, a mass balanced EwE model developed by Lees and Mackinson (2007) that describes the Irish Sea ecosystem in the early 1970s was used as the foundation for the Sellafield model. However, aspects of this model were either beyond the complexity required for the Sellafield model or not descriptive enough and a number of changes were made. The Lees and Mackinson Irish Sea model contains a total of 53 functional groups which was reduced to 43 in the Sellafield model as discussed below.

Three model groups, cod (*Gadus morhua*), haddock (*Melanogrammus aeglefinus*) and plaice (*Pleuronectes platessa*), were separated into two age classes (adult and juvenile). These age-class separations were not necessary for our purposes and these species were instead combined into single species groups in the Sellafield model. Muir et al. (2017) and Tierney et al. (2017a) describe ^{14}C activities in three fish species; dab (*Limanda limanda*), ling (*Molva molva*) and herring (*Clupea harengus*), which are not individually specified in the Irish Sea model. Using species information described in Lees and Mackinson (2007), dab was separated from the "medium flatfish" functional group, ling extracted from "other large demersals", and herring from "other small pelagic planktivorous fish". The functional groups, small, medium and large flatfish were combined into the singular "other flatfish" group. Likewise, a single functional group called "other demersals" was created by combining bass, seatrout, gurnards, mullet, other large demersals, other large gadoids, other small demersals and other small gadoids. The Irish Sea model contained four zooplankton groups (herbivorous, omnivorous, carnivorous and gelatinous), which were also

combined to form a single zooplankton group. Where groups were combined, biomass values were summed and other input parameters from Lees and Mackinson (2007) were calculated as a proportion of the biomasses of the previously existing groups. Where new groups were extracted, biomasses and other input parameters were taken as described in Lees and Mackinson (2007).

Tierney et al. (2017b) describe ^{14}C activities in 3 marine mammal species: harbour porpoise (*Phocoena phocoena*), harbour/common seal (*Phoca vitulina*) and grey seal (*Halichoerus grypus*). None of these species are specified in the Irish Sea model, which contains the mammal functional groups: baleen whale, toothed whale and seals. The description of marine mammals in the Irish Sea model was the focus of a model re-structuring by Hernandez-Milian (2014). Following this, the existing Irish Sea mammal groups were removed and five new functional groups were added for specific species: bottlenose dolphin (*Tursiops truncates*), harbour porpoise, minke whale (*Balaenoptera acutorostrata*), common seal and grey seal. Input parameters including biomass, P/B, Q/B and diet for these functional groups were taken from Hernandez-Milian (2014).

At the base of the food web, primary producers, particularly phytoplankton, were key functional groups in the Sellafield model as ^{14}C enters the food web through uptake by primary producers during photosynthesis. Phytoplankton biomass and P/B were re-calculated using the formula from Gowen and Bloomfield (1996) and primary productivity estimates from Gowen et al. (2000) of 97 g/m^2 for the coastal Irish Sea. This resulted in an increase in biomass (from 9.7 to 13.8 t/km^2) and a reduction in the P/B value (from 152.5 to 70.1 year^{-1}).

Ecopath also requires diet estimates of each functional group and the diet matrix was largely carried over from the Irish Sea model. Where groups were combined, new diet estimates were calculated from previous diets as a function of each group's biomass. Where new groups were created, the diet was assumed to be the same; for example, herring and “other small pelagic planktivorous fish” have the same diet. Diets for the new mammal groups were taken from Hernandez-Milian (2014). The diets for two functional groups, small sharks and monkfish (*Lophius piscatorius*), were edited for better definition: small shark diet was updated according to Ellis et al. (1996) and monkfish diet was updated according to Crozier (1985). The Sellafield model input parameters and diet matrix are included in the Appendix (Tables A.1 and A.2).

The Irish Sea model contained nine fisheries which were retained in the Sellafield model. Landings and discards of these fisheries were corrected for the new and combined functional groups but no other changes were made.

2.2. PREBAL and balancing

After the described changes to the model were made, model assumptions were tested following a set of pre-balance diagnostics (PREBAL) described by Link (2010). PREBAL checks that the ecosystem model makes ecological and thermodynamic sense by checking the slopes of biomass ratios and other data input against trophic levels. There were no significant issues with the Sellafield model, however, the annual P/B ratios for dab (2.4) and other flatfish (2.2) did appear to be high and conversely, the P/B ratios for herring (0.7) and “other small pelagic planktivorous fish” (0.7) appeared to be relatively low. No changes were made to the input parameters for these groups following PREBAL, however, the groups were highlighted again during model balancing.

The Ecopath model must be mass-balanced after entering the input parameters (Heymans et al., 2016). The Sellafield model was initially imbalanced and several parameters were subsequently corrected, as explained below. Increases in biomass for whiting (*Merlangius merlangus*; 8.5%), and lobster and large crabs (12.2%), are within the biomass estimates reported by Lees and Mackinson (2007). The biomass increases to the “epifaunal mesobenthos” (0.27%), and “prawn and shrimp” (1.8%), are negligible relative to the changes in biomass made by Lees and Mackinson (2007) when balancing the Irish Sea model. Large differences were found in the Irish Sea model between the initial biomass values used and the balanced biomasses for monkfish, flatfish (small, medium and large), Nephrops and zooplankton groups. Biomasses were estimated in Ecopath for monkfish, dab, other flatfish, Nephrops and zooplankton by setting ecotrophic efficiency (EE) to 0.95 for these groups. This assumes that the model uses all but 5% of the production of that group and Ecopath can estimate a biomass based on this assumption. In addition, the P/B ratios for dab and other flatfish were estimated in Ecopath by setting the production/consumption (P/Q) ratio for these groups to 0.2. These changes were made based on best practices described by Heymans et al. (2016). As herring P/B had been identified as being relatively high, it was re-calculated using fishing mortality (F) from Lees and Mackinson (2007) and natural mortality (M) from FishBase (Froese and Pauly, 2016) as P/B is equal to total mortality (Z). Mackerel Q/B was corrected using default values from FishBase including a mean temperature of 10 °C. Corrections were also made to the diet matrix for model balancing and the most significant of these was the reduction in consumption of discards which was relatively high in the Irish Sea model, e.g. the proportion of discards in the diet of Nephrops was reduced from 0.5 to 0.03. This was balanced by increasing the proportion of particulate organic matter in diets. A further important change was a substantial increase in the proportion of polychaetes in dab diet as described by (Gibson and Ezzi, 1987). All changes made to both the input parameters and the diet matrix for model balancing are shown in the Appendix (Tables A1 and A2).

2.3. Ecospace

To accurately predict uptake of Sellafield-derived ^{14}C, the Sellafield model had to be spatially resolved. In Ecospace, the biomass (B) of a functional group for a specific grid-cell at time t can be expressed as:

$$\frac{dB}{dt} = (I + g.C) - (Z + E).B$$

where I is the total immigration rate from surrounding cells, g is the net growth efficiency, C is food consumption rate, Z is total instantaneous mortality rate, and E is total instantaneous emigration rate (Walters et al., 1999).

Due to the net northward dispersion of ^{14}C and the available data for the West of Scotland (Tierney et al., 2017a, 2017b) the Ecospace base-map of the Sellafield model, produced in ArcGIS, encompasses part of the West of Scotland marine environment as well as the Irish Sea (Fig. 1). Base-map grid resolution was 5 km with boundaries at approximately 56° 45′ N (northern boundary), 02° 45′ W (eastern boundary), 53° 15′ N (southern boundary) and 7° 15’ W (western boundary). The base-map covers key sites in both the Irish Sea and West of Scotland, used in studies concerning ^{14}C in the environment and biota (Muir et al., 2017; Tierney et al., 2017a, 2017b).

The recently introduced contaminant map layer in Ecospace allows the user to input contaminant concentrations across the base-map. This can now be used to select a specific point source for a contaminant, which is limited to the base-map resolution. A

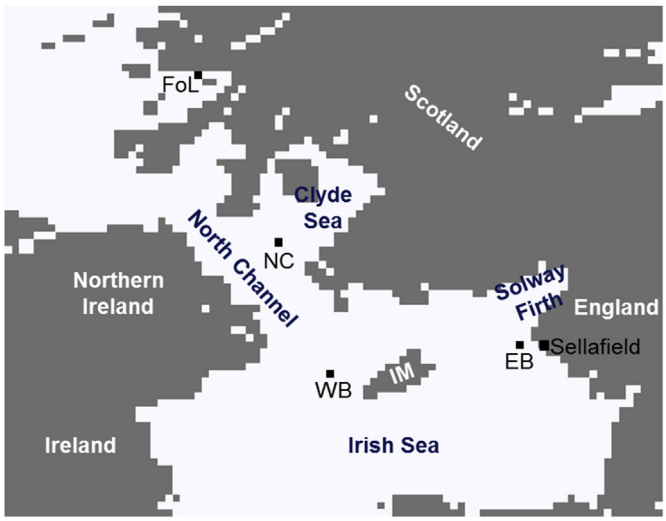

Fig. 1. Annotated Sellafield model Ecospace base-map with 5 × 5 km resolution (IM = Isle of Man). Grid cells representing sample stations (EB, WB, NC and FoL) from Muir et al. (2017) and Tierney et al. (2017a) are also shown.

contaminant can be dispersed in Ecospace using the base dispersal rate for the first detrital group listed in the model. The base dispersal rate is used to set the rate with which organisms in the ecosystem will disperse due to random movements where the default is 300 km year^{-1} but this can also be applied to a contaminant. In addition, a more realistic dispersion pattern can be created using the advection map layer by inputting x (east-west) and y (north-south) velocity data at the base-map resolution. The spatial-temporal framework, a GIS-based data exchange framework built on DotSpatial (Steenbeek et al., 2013; Ames et al., 2012), allowed a time-series of variable ocean velocity data to be input to the running model. Month averaged x and y velocities at 7 km grid resolution from a hind-cast model of the north-east Atlantic, for the period January 1985 to June 2014 (most recent data available at the time of study), were sourced from the European Commission Copernicus Marine Environment Monitoring Service (http://marine.copernicus.eu). Data for the model area were extracted and velocities were depth averaged. The data were extrapolated over the base-map 5 km grid resolution and a time-series of map files (ASCII) for x and y velocities on monthly time steps were produced. These data files were read into Ecospace using the spatial-temporal framework (Steenbeek et al., 2013) to create advection fields and the model was run on monthly time-steps. Phytoplankton and zooplankton dispersion, as well as contaminant dispersion, were linked to model advection.

2.4. Ecotracer

The iteration of EwE used for the Sellafield model contained changes to the Ecotracer component that will be included in the next release of EwE (EwE 6.6, to be released summer 2018). When running Ecotracer in Ecosim (non-spatial contaminant modelling) it is possible to link contaminant inputs to a data time-series. To do this for a point source in Ecospace, a new Ecotracer function was added which allows variable contaminant input at specified grid cells, limited to the base-map resolution. For the Sellafield model, this means that ^{14}C input was in a 25 km^2 area where the Sellafield pipelines end. This input was made as total monthly ^{14}C discharge activity from Sellafield in Becquerels (Bq).

Other input parameters in Ecotracer include: initial contaminant concentration, contaminant concentration in immigrating biomass, direct uptake, physical decay rate, proportion of contaminant excreted and metabolic decay rate (Table 1). Initial contaminant concentrations must be set for both the environment and the functional groups. Sellafield ^{14}C discharges are in addition to an existing "background" ^{14}C activity from natural production and atmospheric atomic weapons testing. The initial contaminant concentration in the Sellafield model was set at zero and, as the only input was from Sellafield ^{14}C discharges, any increase in functional group contaminant concentration shows net ^{14}C enrichment in excess of background.

Direct uptake is the rate at which a functional group takes up the contaminant from the environment. ^{14}C is discharged to the marine environment as DIC and primary producing organisms incorporate dissolved inorganic ^{14}C, through fixation of carbon during photosynthesis into soft tissue. For phytoplankton, direct uptake was calculated as the rate at which phytoplankton photosynthesise as it is assumed that ^{14}C uptake is identical to stable carbon uptake. Following Walters and Christensen (2017) this can be expressed as:

$$Direct\ uptake = u_i/B_i/C_0$$

Where u_i is the mass of carbon intake by primary producer i, B_i is the biomass of primary producer i and C_0 is the DIC concentration. Phytoplankton ^{14}C uptake was calculated using the primary productivity estimate of 97 g m^{-2} for the coastal Irish Sea (Gowen et al., 2000), the calculated biomass 13.8 t km^{-2} and an estimated DIC concentration of 30 mg l^{-1}, taken from the upper limit of typical DIC concentrations in seawater of 24–30 mg C l^{-1} (Chester, 1990). Primary productivity rates for the other primary producers, seaweed and microflora were estimated by back calculating from the model biomass using formula from Gowen and Bloomfield (1996). Productivity rates of 450 g m^{-2} (seaweed) and 230 g m^{-2} (microflora) were then used to calculate direct uptake for these groups. Contaminant uptake for consumer groups is a function of the contaminant concentration in their diet, their consumption rate and their mortality (Walters and Christensen, 2017).

There are two excretion parameters for each functional group. The proportion of contaminant excreted is the proportion not assimilated into the biomass and so passes straight into the detritus group. The default annual unassimilated consumption for consumer groups in the Ecopath parameters is 0.2 and this was copied for the proportion of contaminant excreted in the Sellafield model as ^{14}C acts as a tracer of stable carbon and, therefore, energy transfer in an ecosystem.

The metabolic decay rate is the rate at which assimilated contaminant is released back into the environment (see "excretion" in Walters and Christensen, 2017). The carbon weight ^{14}C activity (Bq per mass C) of marine primary producers is in equilibrium with the DIC ^{14}C activity. Therefore, the metabolic decay rate for primary producers can be calculated where the equilibrium ratio of ^{14}C in a primary producer is equal to the environmental concentration. For example, when the DIC ^{14}C activity is at background (approximately 249 Bq kg^{-1} C), the ^{14}C activity in a primary producer is expected to be the same. Under these conditions the metabolic decay rate can be expressed as:

$$Metabolic\ decay\ rate = D_i.C_0 \Big/ \left(\frac{C_i}{B_i}\right)$$

where D_i is the direct uptake rate for the primary producer i, C_0 is the ^{14}C concentration in the environment, C_i is the ^{14}C

Table 1
Sellafield model Ecotracer parameters.

Group Name	Initial Conc. (t/t)	Direct uptake rate (t/t/t/year)	Proportion excreted	Metabolic decay rate (/year)
Bottlenose Dolphin	0	0	0.2	6.836
Harbour Porpoise	0	0	0.2	6.836
Minke Whale	0	0	0.2	7.980
Common Seal	0	0	0.2	11.520
Grey Seal	0	0	0.2	11.520
Seabirds	0	0	0.2	65.056
Large Sharks	0	0	0.2	2.226
Small Sharks	0	0	0.2	6.804
Basking Sharks	0	0	0.2	2.890
Skates and Rays	0	0	0.2	11.200
Cod	0	0	0.2	2.375
Haddock	0	0	0.2	4.353
Plaice	0	0	0.2	3.146
Whiting	0	0	0.2	1.534
Sole	0	0	0.2	1.201
Monkfish	0	0	0.2	1.193
Dab	0	0	0.2	1.825
Other Flatfish	0	0	0.2	2.314
Dragonets	0	0	0.2	2.583
Mackerel	0	0	0.2	3.106
Ling	0	0	0.2	1.156
Other Demersals	0	0	0.2	2.133
Herring	0	0	0.2	4.059
Other Planktivorous Fish	0	0	0.2	4.486
Sandeels	0	0	0.2	2.483
Epifaunal Macrobenthos	0	0	0.2	4.983
Epifaunal Mesobenthos	0	0	0.2	5.436
Infaunal Macrobenthos	0	0	0.2	8.085
Infaunal Mesobenthos	0	0	0.2	6.728
Infauna (Polycheate)	0	0	0.2	6.138
Lobster and Large Crabs	0	0	0.2	3.393
Nephrops	0	0	0.2	3.164
Cephalopods	0	0	0.2	10.019
Prawns and Shrimp	0	0	0.2	4.155
Sessile Epifauna	0	0	0.2	6.198
Meiofauna	0	0	0.2	30.750
Zooplankton	0	0	0.2	25.476
Seaweed	0	0.002	0	6.000
Microflora	0	0.020	0	58.700
Phytoplankton	0	0.002	0	7.014
Particulate Organic Matter	0	0	0	n/a
Dissolved Organic Matter	0	0	0	n/a
Discards	0	0	0	n/a

concentration in primary producer i and B_i is the biomass of primary producer i. The metabolic decay rate was calculated this way for all three primary producers in the Sellafield model. For consumer groups, the metabolic decay rate was assumed to be equal to the respiration rate/biomass which were calculated in the Ecopath component during model balancing.

A contaminant physical decay rate parameter was added to the Ecotracer module in the version used here. This can be set for both the environment and each functional group. For radionuclides, this is the physical radioactive decay rate, meaning that in EwE, biological decay and physical radioactive decay are two separate parameters. ^{14}C has a long half-life of 5730 years and the impact of radioactive decay on a model running over several decades is negligible, and so, physical decay rate was set at zero. As the Ecopath food web model contained no immigration, the contaminant concentration in the immigrating biomass could also be set to zero for every functional group.

Muir et al. (2017) and Tierney et al. (2017a) describe ^{14}C activities at numerous sites including 4 main stations (Fig. 1) located in the Irish Sea east basin (EB), Irish Sea west basin (WB), North Channel (NC) and Firth of Lorn (FoL). Model base-map grid cells at these site locations or, in the case of FoL, as close as possible, were labelled as different model regions in Ecospace and data specific to these regions were extracted from EwE. Model data analyses were conducted and map figures were produced using R (R Development Core Team, 2016) and the R package "ggmap" (Kahle and Wickham, 2013) used to overlay model predicted data over Google satellite maps. Model predictions are only given where ^{14}C enrichment is at least 1 Bq kg^{-1} C and all observed ^{14}C activities are given as net activities (i.e. background subtracted).

3. Results and discussion

3.1. ^{14}C dispersion

Although advection was the dominant control on the general direction and extent of model ^{14}C dispersion, contaminant base dispersal rate had an observed impact (Fig. 2). As ^{14}C uptake by primary producers is limited to the ^{14}C activity of the environment (or DIC ^{14}C activity) for a given cell, the physical dispersion of Sellafield ^{14}C is a key mechanism. Studies examining the dispersion of other highly soluble radionuclides discharged by Sellafield (e.g. ^{134}Cs, ^{137}Cs and ^{99}Tc) have estimated transit times from Sellafield to the North Channel of between 3 months and 1.8 years (Jefferies

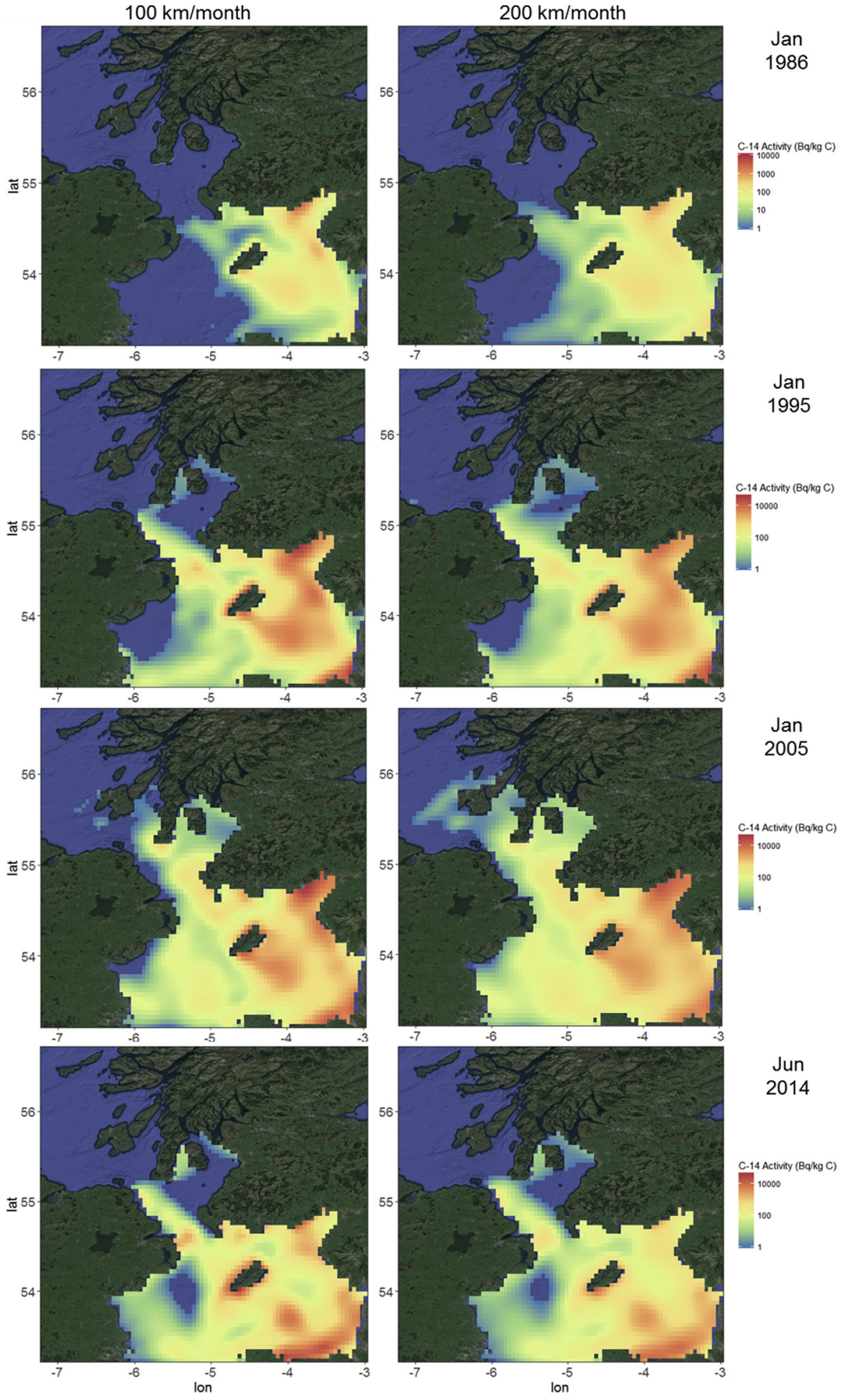

Fig. 2. Modelled DIC ^{14}C activities (calculated from modelled environmental ^{14}C activity) for four different months using two different base dispersion rates: 100 km per month (left) and 200 km per month (right). Note that the ^{14}C activity scale increases to 40,000 Bq kg^{-1} C from January 1995 to account for higher predicted activities particularly at the lower dispersion rate.

et al., 1973; Kershaw and Baxter, 1995; Kershaw et al., 2004). Similarly, transit times of between 3 months and 1 year were predicted by the model developed by Dabrowski and Hartnett (2008). Using a base dispersal rate of at least 100 km per month resulted in model ^{14}C reaching the North Channel within 1 year (Fig. 2). As the distance between Sellafield and the North Channel is approximately 110 km, it is apparent that model dispersion of ^{14}C is limited by both advection and uptake by primary producers.

Increasing the base dispersal rate does increase maximum dispersal extent, though this increase does not appear to be substantial. It does reduce the maximum DIC ^{14}C activities predicted in pockets where ^{14}C appears to accumulate, e.g. the Solway Firth. This accumulation, particularly at lower base dispersal rates, causes activities to increase to levels which have not been observed in previous studies. For example, the model predicted ^{14}C activities above 30KBq kg^{-1} C between 2001 and 2006 when using a base dispersal rate of 100 km per month. However, an increase in base dispersal rate to 200 km per month, limited maximum model DIC activities to less than 20 KBq kg^{-1} C. There are no reported DIC ^{14}C activities for the period of peak predicted activity (2001–2006) and, therefore, no available data for DIC activities in areas such as the Solway Firth where a significant accumulation of ^{14}C was predicted for this period.

The highest reported net DIC ^{14}C activities are approximately 8550 Bq kg^{-1} C in 1995 (Cook et al., 1998) and 4500 Bq kg^{-1} C in 1997 (Cook et al., 2004), at sites relatively close to Sellafield. Using a time-series of DIC ^{14}C activities for a site in the vicinity of Sellafield for the period 1989 to 1999 (Cook et al., 2004), it is shown that the range of activities predicted by the model when using a base dispersal rate of 200 km per month was similar to the observed range through time (Fig. 3). Although the specific measured and predicted activities do not generally align, it is important to recognise that model ^{14}C activities are predicted per km^2 (for a 25 km^2 cell) per month, whereas measured DIC samples were taken from a specific day and location on the coastline. Model dispersion of DIC ^{14}C could be improved with further measurements at sites such as the Solway Firth to address uncertainty in dispersion. To illustrate model dispersion of dissolved inorganic ^{14}C in the environment a video component (Video 1) is available and accompanies the electronic version of the manuscript.

Supplementary video related to this article can be found at https://doi.org/10.1016/j.envsoft.2018.01.013.

In addition to the Solway Firth, accumulation of ^{14}C occurs in the south-east Irish Sea and around the Isle of Man. Circulation models have described a significant seasonal southward flow in the Irish Sea (Dabrowski and Hartnett, 2008; Dabrowski et al., 2010) creating a backwater in the south-east Irish Sea. This could result in the area around Liverpool Bay being a significant sink for radionuclides released from Sellafield (Dabrowski and Hartnett, 2008). An increase in the radionuclide inventories of saltmarsh sediments in areas including the Solway Firth has previously been suggested (MacKenzie et al., 2004). However, an accumulation of Sellafield radionuclides in the water column of the Solway Firth and also around the Isle of Man has not been previously detected and the general northward movement of water continuously flushed the Isle of Man coastline in circulation models (Dabrowski and Hartnett, 2008). Although accumulation of ^{14}C in these areas could occur, any accumulation in concentration may not occur to the same extent predicted by the EwE model. Greater retention of ^{14}C at these sites will result in reduced dispersion to more distant areas.

The fact that modelled ^{14}C dispersion does not significantly penetrate the Scottish west coast, suggests that model retention in the Irish Sea is too high. Previous studies have shown that a significant proportion of Sellafield discharges are dispersed around the Scottish coastline (Gulliver et al., 2001; Tierney et al., 2016. 2017a). The consequence of using depth averaged advection in our study is that the necessary complex hydrodynamics to drive dispersion at this regional scale may not be well addressed in this model. At coastal areas, such as the Solway Firth, dispersion will be complicated by freshwater input and non-uniform current direction at different depths which would reduce the overall retention of dissolved ^{14}C at these sites. Using depth averaged advection means that dissolved ^{14}C can be trapped and accumulate exponentially at sites if advection is directed towards the coastline, although this is significantly reduced by increasing the base dispersal rate.

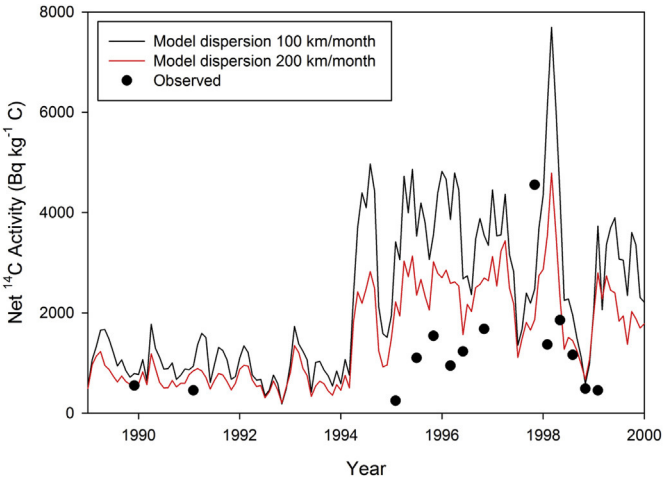

Fig. 3. Modelled DIC ^{14}C activities between 1989 and 2000 from offshore Sellafield compared to activities observed in Cook et al. (2004).

Dispersion is also limited by data and map resolution. The velocity data used had a grid resolution of 7 km so any local physical dynamics were lost. The 5 km base-map grid resolution meant that many features of the UK coastline were not well defined, including the loss of several islands on the Scottish west coast that are connected to the mainland in the model.

3.2. ^{14}C ecological fate

Muir et al. (2017) reported ^{14}C activities for DIC and a number of species at sites in the Irish Sea east basin (station EB) and west basin (station WB) in June 2014. Model ^{14}C activities at EB in June 2014 were significantly over-predicted compared to observed activities when using a low dispersal rate (100 km per month) but a higher base dispersal rate (200 km per month) brought the predicted and observed activities significantly closer (Fig. 4). Trends in the observed data were replicated by the model. Phytoplankton and zooplankton ^{14}C activities were relatively low compared to benthic species and dab ^{14}C activity was the highest; although a large range in observed dab activity (499–763 Bq kg^{-1} C) meant that the average dab activity (631 Bq kg^{-1} C) was less than the infaunal macrobenthos (704 Bq kg^{-1} C). The model did not capture this high infaunal macrobenthos ^{14}C activity relative to most other groups. The observed infaunal macrobenthos activity comes from green spoon worm (*Maxmuelleria lankesteri*) tissue and this species is known to have an important role in the redistribution of other Sellafield-derived radionuclides in bottom sediments (Hughes et al., 1996; Kershaw et al., 1983, 1984, 1999). Its inclusion as a

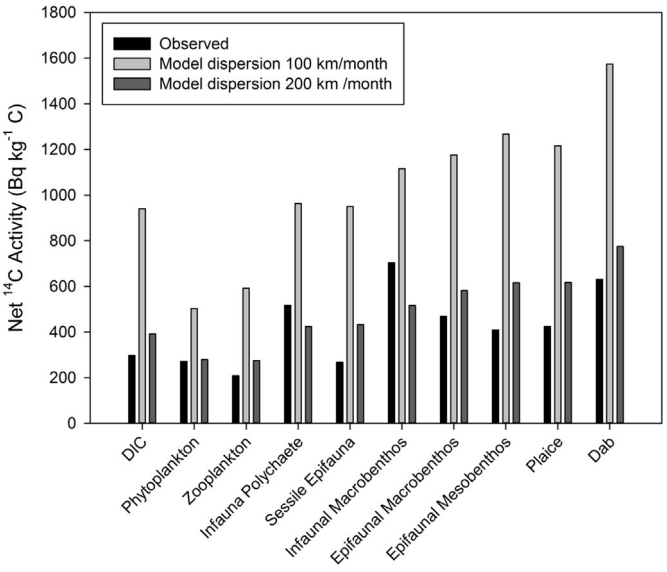

Fig. 4. Modelled DIC and selected functional group ^{14}C activities for June 2014 at the Irish Sea east basin station (EB) compared to activities observed in Muir et al. (2017).

separate species in the model was considered, however, this was deemed to be challenging due to limited ecological data.

Station WB is more complex due to highly variable reported ^{14}C activities between species (Muir et al., 2017). Typically, both high and low dispersion rates under-predicted the observed higher activities (in polychaetes, epifaunal macrobenthos and dab) and over-predicted the observed lower activities (e.g. phytoplankton and zooplankton; Fig. 5). However, the main observed trends were again predicted. As for EB, plankton ^{14}C activities were significantly lower than other functional groups and dab activity was again predicted to be the highest. The relatively high ^{14}C activity observed in polychaetes (405 Bq kg^{-1} C) was due to the higher observed net activity of the predatory species *Aphrodita aculeate* (740 Bq kg^{-1} C) whereas the average activity of other polychaete species was lower (69 Bq kg^{-1} C) and similar to the model predicted activity of 59 Bq kg^{-1} C. The observed epifaunal macrobenthos activity was also relatively high (488 Bq kg^{-1} C) and not captured by the model. Similar to the polychaete group, the model functional group epifaunal macrobenthos was made up of numerous species and the observed ^{14}C activity was comprised from an average of starfish species only and may not accurately represent the entire functional group. Both these cases indicate that model functional groups were not well defined in some instances, as the addition of a predatory species to a functional group is not best practice (Heymans et al., 2016).

A number of ^{14}C activities, across a range of species, were reported by Tierney et al. (2017a) for two sites in the West of Scotland marine environment; the North Channel (station NC) and Firth of Lorn (station FoL). Due to northward dispersion of ^{14}C being constrained in the model, as a result of Irish Sea retention of ^{14}C being too high, the model under-predicts activities at these sites relative to the observed activities. Additionally, the connection of several islands to the Scottish mainland, due to the 5 km base map resolution, blocked important channels in the West of Scotland area including to the south of the Firth of Lorn (preventing direct northward dispersion of ^{14}C to this area) and much of the Firth of Lorn itself. The lack of penetrative northward dispersion of ^{14}C resulted in the model showing no ^{14}C enrichment at FoL in 2014, although a small enrichment in DIC and benthic species was observed (Tierney et al., 2017a). The model only predicted a slight enrichment (1–2 Bq kg^{-1} C) in DIC and some functional groups at FoL between 2005 and 2009. At station NC, the observed trend of low plankton activities and higher benthic activities was again replicated in June 2014 (Fig. 6). As observed, whiting activity was predicted to be higher than other groups and repeated the theme where the group with the highest modelled trophic level also had the highest activity (see dab for Irish Sea sites). However, the comparatively high activity observed in whiting at the NC station was interpreted as being likely due to northward migration of whiting which had foraged in the Irish Sea (Tierney et al., 2017a).

The issues discussed with the model ^{14}C dispersion meant that predicted activities for harbour porpoises did not typically align with the activities reported by Tierney et al. (2017b). It should also be noted that although harbour porpoise is a resident species, and observed ^{14}C activities indicate a high feeding fidelity (Tierney

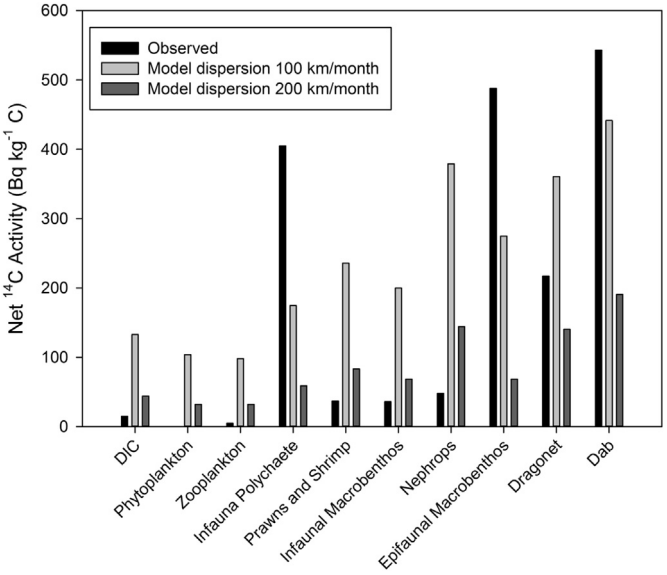

Fig. 5. Modelled DIC and selected functional group ^{14}C activities for June 2014 at the Irish Sea west basin station (WB) compared to activities observed in Muir et al. (2017).

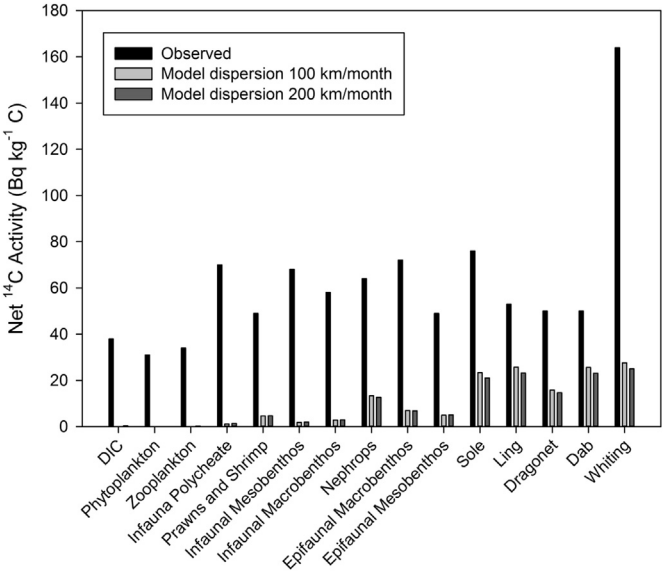

Fig. 6. Modelled DIC and selected functional group ^{14}C activities for June 2014 at the North Channel Station (NC) compared to activities observed in Tierney et al. (2017a).

et al., 2017b), these are animals that can traverse the modelled area and single measurements from a stranded individual is unlikely to represent the average activity across the population in that area. Predicted trends through time do, however, appear to replicate the observed trends as illustrated by comparing predicted harbour porpoise ^{14}C activities in four different years (1993, 2002, 2004 and 2014) with the observed activities for those years (Fig. 7). Both predicted and observed ^{14}C activities show very low ^{14}C activities of between 0 and 10 Bq kg^{-1} for West of Scotland porpoises north of the North Channel in 1993, with activities significantly higher in the south-east Irish Sea. Peak discharges between 2001 and 2005 increased porpoise ^{14}C activity in the.

North-east Irish Sea and activities were lower in the North Channel and Clyde Sea. Clyde Sea ^{14}C activities were lower in 2014 but activities in the North Channel remained relatively higher and the highest activities were found in the south-east Irish Sea.

The Sellafield model illustrates that ecosystem uptake of ^{14}C for a specific area is controlled by the DIC ^{14}C activity in that area and, therefore, the dispersion of changeable Sellafield ^{14}C discharges through time (Fig. 8). Phytoplankton and, subsequently, zooplankton ^{14}C activities closely mirror changes in the DIC ^{14}C activity. As ^{14}C transfers to higher trophic levels are not immediate, there is a delayed response to ^{14}C activities which has a smoothing effect on predicted activities through time. Modelled ^{14}C activities for stations EB, WB and NC in June 2014 show a general trend of increasing activity with increasing trophic level (Figs. 4–6). This is not due to bioaccumulation but rather the lag effect in ^{14}C transfer to higher trophic levels, culminating in top predators such as harbour porpoise. The very low ^{14}C discharge activity in June 2014 caused DIC and plankton activities to drop at station EB whilst other functional group activities remained higher due to uptake of previously higher activities. Variable dispersion of ^{14}C to station WB

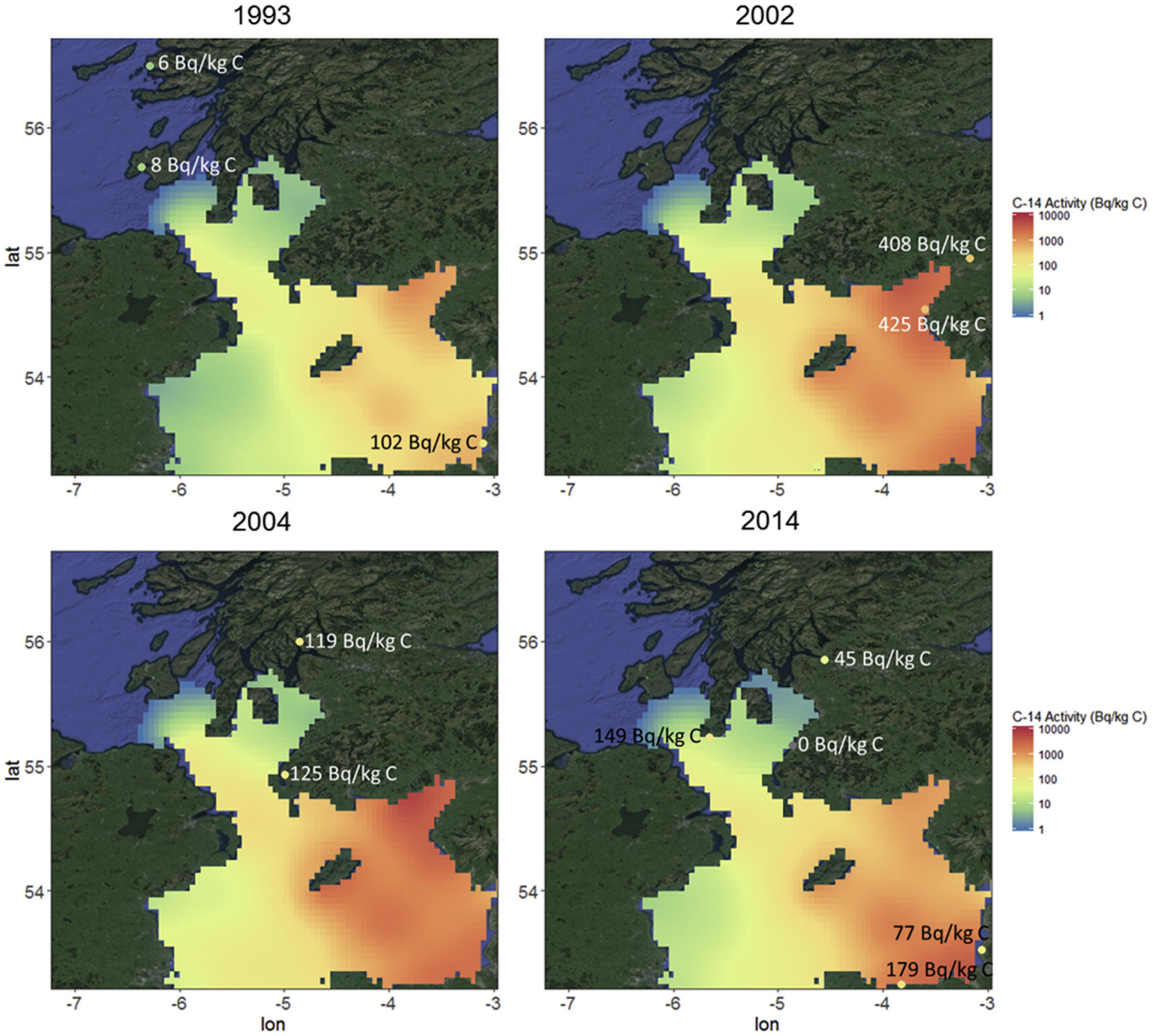

Fig. 7. Averaged modelled harbour porpoise ^{14}C activities from 1993, 2002, 2004 and 2014 compared to measured activities observed in Tierney et al. (2017b) shown as dots with annotated activity. Several of the observed activities were obtained from samples retrieved within river estuaries and sea lochs which were not modelled.

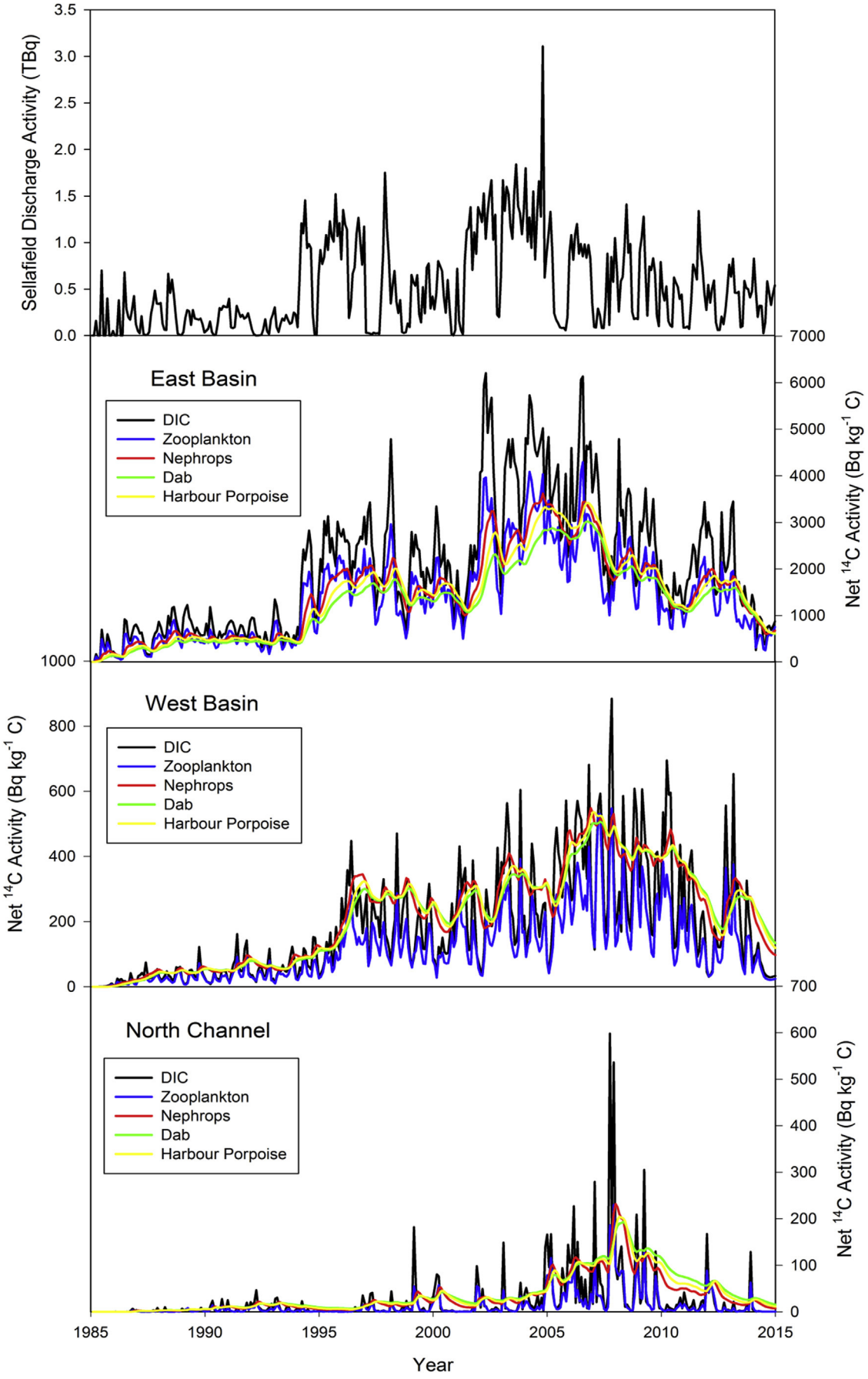

Fig. 8. Monthly Sellafield ^{14}C discharge data input to the model (top). Modelled DIC and selected functional group ^{14}C activities at the east basin (EB), west basin (WB) and North Channel (NC) stations for the duration of the model run using a high base dispersion rate (200 km per month).

resulted in DIC and plankton activities decreasing significantly below the ^{14}C activities of other species in June 2014. After a peak in DIC activity at station NC in 2007, the activities at higher trophic levels gradually declined, but not to below the significantly reduced plankton activities. This mechanism, which likely caused the higher observed ^{14}C activities in benthic species, was suggested by Muir et al. (2017) and Tierney et al. (2017a) who described an integrated ^{14}C activity in older living organisms occupying higher trophic levels. It was also identified through analysis of marine mammal ^{14}C activities alone (Tierney et al., 2017b) where mammal ^{14}C activities correlated significantly with total Sellafield discharges for 24 months prior to stranding. As shown by model results, this means that the ^{14}C activity of an organism is not only dependent on the discharge activity and the dispersion of ^{14}C, which can be highly variable, but is also dependent on the trophic level that the organism feeds at. Feeding at lower trophic levels will result in a species having a highly variable ^{14}C activity through time. Species that feed at higher trophic levels will have ^{14}C activities that are not dependent on the immediate environmental activity and could be significantly more or less enriched in ^{14}C relative to the environment they inhabit. To illustrate the differences in ^{14}C activities spatially and temporally at different trophic levels, a video component (Video 2) is available and accompanies the electronic version of the manuscript.

Supplementary video related to this article can be found at https://doi.org/10.1016/j.envsoft.2018.01.013.

3.3. Advantages and limitations

As discussed, the EwE approach accurately demonstrates a number of the observed trends in ^{14}C activities and reproduces the observed transfer of ^{14}C through the marine food-web, after initial uptake by primary producers relative to the environmental ^{14}C activity. It can, therefore, provide a tool which is capable of predicting the ecological uptake of radioactive contamination, or other environmental contaminants (i.e. trace metals), if the environmental concentrations were accurately provided. Predicted activities for a specific functional group are limited by how well each functional group and their ecology are defined in the model. Diet is a key factor in an organisms ^{14}C activity, and diet description data should be revisited and improved (where possible) for the Sellafield model. A major advantage of EwE is that it can predict general trends for contaminant concentrations in non-specific functional groups, or specific contaminant concentrations in individual species. For example, if the aim was to determine the transfer of ^{14}C or other radionuclides between different benthic species and the sediment, then the functional groups describing these species should be further developed. Discrepancies between observed and predicted activities for benthic species would be better resolved by incorporation of a well-defined microbial loop in the model.

Modelling ^{14}C dispersion within the EwE framework significantly reduces far-field dispersion beyond the Irish Sea in comparison to observed data, and appears to result from increased retention of ^{14}C at specific areas within the Irish Sea. As this study aimed to model the general patterns of ^{14}C dispersion, the velocity and base-map resolutions are appropriate, nevertheless, using depth averaged advection over simplifies the localised oceanographic conditions. In future work, this could be overcome by using a 3-dimensional physical-transport model to disperse ^{14}C in the environment. By using the same approach to which velocity data were input to Ecospace in this study, employing the spatial-temporal framework (Steenbeek et al., 2013), depth-averaged ^{14}C activity/concentration fields predicted by the physical-transport model could be applied instead.

This study did not consider ecosystem shifts (e.g. changes in species biomass and the knock-on effects) through time. However, if a model contamination study for an area covers an extensive period of time, then changes in the ecosystem which could affect contaminant concentration in the ecology should also be modelled in EwE. The Sellafield ^{14}C model and observed ^{14}C activities show that the ^{14}C activity for a functional group/species is dependent on the trophic level it feeds upon. Most ecosystems, in general, and the Irish Sea specifically, have undergone significant changes over the past century due to changes in the fishing/hunting pressures and climate, which result in species changing their foraging behaviour and the prey they feed on. This would affect the ^{14}C activity of a species and, if the contaminant was subject to bioaccumulation, this could lead to additional model complexities. Future work should consider this and, for ^{14}C, seek to address changes in ecosystem uptake due to seasonal variation in primary productivity.

4. Conclusions

This study modelled the ecosystem uptake and ecological fate of Sellafield ^{14}C discharged to the UK marine environment using the EwE software. The advantages of the EwE approach were illustrated in capturing observed trends in ^{14}C activities for species at specific locations and through time. In addition, the model data aids understanding of ^{14}C transfer processes through the food-web. ^{14}C does not bio-accumulate, although higher activities have been observed at higher trophic levels. The Sellafield model illustrates that changes in environmental ^{14}C activities will directly and immediately impact species activity at lower trophic levels, whereas higher trophic level species' ^{14}C activities are integrated over time. Therefore, species ^{14}C activity will be strongly affected by the trophic level from which it feeds.

Limitations in the model's ability to use advection data to disperse ^{14}C through the marine environment meant that the specific ^{14}C activities predicted for some areas, such as the West of Scotland, did not compare well with observed activities. Further measurements of DIC ^{14}C activities, such as the Solway Firth where the model predicts an accumulation of Sellafield ^{14}C, would reduce uncertainty in dispersion patterns.

The effectiveness of EwE for modelling the ecological fate of contaminants in the environment has been underrepresented despite the wide use of the EwE approach to ecosystem modelling. Recent developments in the software were utilised in this study. Further refinements, such as coupling this approach with better resolved contaminant dispersion, could be used to help address the ecological fate of a wide range of contaminants including radionuclides.

Acknowledgements

This work was completed as part of the LO-RISE (Long-lived Radionuclides in Surface Environments; NE/L000202/1) consortium under the NERC RATE programme (Radioactivity and the Environment), co-funded by the Environment Agency and Radioactive Waste Management Ltd. This study has been conducted using E.U. Copernicus Marine Service Information.

Appendix

A.1 Sellafield model functional groups and balanced input parameters; biomass, production/biomass (P/B), consumption/biomass (Q/B), ecotrophic efficiency (EE), production/consumption (P/Q) and unassimilated consumption. Values used before balancing are shown in brackets, where applicable.

Group name	Biomass (t/km^2)	P/B (/year)	Q/B (/year)	EE	P/Q	Unassimilated consumption
Bottlenose Dolphin	0.0016	0.2	8.67			0.2
Harbour Porpoise	0.0105	0.2	8.67			0.2
Minke Whale	0.0893	0.02	10			0.2
Common Seal	0.0005	0.1	14.55			0.2
Grey Seal	0.004	0.1	14.55			0.2
Seabirds	0.0511	1.075	82.664			0.2
Large Sharks	0.115	0.318	3.18			0.2
Small Sharks	0.288	0.972	9.72			0.2
Basking Sharks	0.0014	0.07	3.7			0.2
Skates and Rays	0.103	1.6	16			0.2
Cod	0.6253	1.3891	4.7051			0.2
Haddock	0.2711	2.4751	8.5356			0.2
Plaice	0.3425	1.3522	5.6234			0.2
Whiting	0.55 (0.507)	0.842	2.97			0.2
Sole	0.16	0.863	2.58			0.2
Monkfish	(0.125)	(1.246)	1.989	0.95	0.2	0.2
Dab	(0.07)	(2.394)	3.042	0.95	0.2	0.2
Other Flatfish	(0.2404)	(2.1757)	3.8572	0.95	0.2	0.2
Dragonets	0.229	1.54	5.154			0.2
Mackerel	1.623	0.414	4.4 (1.73)			0.2
Ling	0.076	1.315	3.089			0.2
Other Demersals	2.4158	1.5384	4.5888			0.2
Herring	1.2131	1.154 (0.727)	6.516			0.2
Other Small Pelagic Planktivorous Fish	2.4262	0.727	6.516			0.2
Sandeels	1.3	1.53	5.016			0.2
Epifaunal Macrobenthos	13	1.661			0.2	0.2
Epifaunal Mesobenthos	8.999 (8.975)	2.062			0.22	0.2
Infaunal Macrobenthos	8.007	2.695			0.2	0.2
Infaunal Mesobenthos	24.773	2.552			0.22	0.2
Infauna (Polycheate)	22.726	3.683			0.3	0.2
Lobster and Large Crabs	0.11 (0.098)	0.783	5.22			0.2
Nephrops	(0.35)	0.73	4.867	0.95		0.2
Cephalopods	0.25	1.981	15			0.2
Prawns and Shrimp	4.925 (4.847)	0.959	6.393			0.2
Sessile Epifauna	7.5	2.066			0.2	0.2
Meiofauna	6.314	18.45			0.3	0.2
Zooplankton	(48.475)	15.2855		0.95	0.3	0.2
Seaweed	75	60				
Microflora	3.92	587				
Phytoplankton	13.83	70.14				
Particulate Organic Matter	50					
Dissolved Organic Matter	50					
Discards	0.309					

A.2 Sellafield model diet matrix. Values used pre-balancing are shown in parentheses, where applicable.

Prey \ predator	Bottlenose Dolphin	Harbour Porpoise	Minke Whale	Common Seal	Grey Seal	Seabirds
Bottlenose Dolphin	0	0	0	0	0	0
Harbour Porpoise	0	0	0	0	0	0
Minke Whale	0	0	0	0	0	0
Common Seal	0	0	0	0	0	0
Grey Seal	0	0	0	0	0	0
Seabirds	0	0	0	0	0	0.0100
Large Sharks	0	0	0	0	0	0
Small Sharks	0.1000	0	0	0.0050	0.0100	0.0010
Basking Sharks	0	0	0	0	0	0
Skates and Rays	0.1000	0	0	0.0790	0.0300	0.0040
Cod	0	0.0059	0	0	0	0.0410
Haddock	0.0593	0.0135	0	0	0	0.0160
Plaice	0.0027	0	0	0.0032	0	0.0050
Whiting	0.0200	0.2130	0	0.0350	0.0300	0.0240
Sole	0.0010	0	0	0.0200	0.0200	0.0070

(*continued on next page*)

(*continued*)

Prey \ predator	Bottlenose Dolphin	Harbour Porpoise	Minke Whale	Common Seal	Grey Seal	Seabirds
Monkfish	0	0	0	0	0	0.0010
Dab	0.0044	0.0066	0	0.0338	0.0182	0.0073
Other Flatfish	0.0186	0.0304	0	0.1025	0.0292	0.0257
Dragonets	0	0	0	0.0371	0.0055	0.0120
Mackerel	0.0126	0.0149	0.2500 (0.4000)	0	0.0950	0.0390
Ling	0.1805	0	0	0.1000	0.0900	0.0130
Other Demersals	0.4615	0.4122	0	0.3873	0.4998	0.1602
Herring	0.0089	0.0563	0.2600 (0.1300)	0.0247	0.0290	0.0020
Other Planktivorous Fish	0.0177	0.1126	0.2800 (0.2600)	0.0493	0.0579	0.0040
Sandeels	0	0.1000	0.0050	0.1038	0.0160	0.1481
Epifaunal Macrobenthos	0	0	0	0	0	0.0521
Epifaunal Mesobenthos	0	0	0	0	0	0.0521
Infaunal Macrobenthos	0	0	0	0	0	0
Infaunal Mesobenthos	0	0	0	0	0	0
Infauna (Polychaete)	0	0	0	0	0	0.1051
Lobster and Large Crabs	0	0	0	0	0.0150	0.0020
Nephrops	0	0	0	0	0.0150	0
Cephalopods	0.0129	0.0343	0.0900	0.0191	0.0395	0
Prawns and Shrimp	0	0	0.1000	0	0	0.1682
Sessile Epifauna	0	0	0	0	0	0
Meiofauna	0	0	0	0	0	0
Zooplankton	0	0	0.0150	0	0	0
Seaweed	0	0	0	0	0	0
Microflora	0	0	0	0	0	0
Phytoplankton	0	0	0	0	0	0
Particulate Organic Matter	0	0	0	0	0	0.0800 (0)
Dissolved Organic Matter	0	0	0	0	0	0
Discards	0	0	0	0	0	0.0200 (0.1000)

Prey \ predator	Large Sharks	Small Sharks	Basking Sharks	Skates and Rays	Cod	Haddock
Bottlenose Dolphin	0	0	0	0	0	0
Harbour Porpoise	0	0	0	0	0	0
Minke Whale	0	0	0	0	0	0
Common Seal	0	0	0	0	0	0
Grey Seal	0	0	0	0	0	0
Seabirds	0	0	0	0	0	0
Large Sharks	0	0	0	0	0	0
Small Sharks	0	0	0	0.0060	0	0
Basking Sharks	0	0	0	0	0	0
Skates and Rays	0	0	0	0.0030	0	0
Cod	0	0	0	0	0.0043	0
Haddock	0	0	0	0	0.0108	0.0074
Plaice	0	0	0	0	0	0
Whiting	0	0	0	0.0080	0.0168	0
Sole	0	0	0	0	0	0
Monkfish	0	0	0	0	0	0
Dab	0	0	0	0.0022	0.0021	0
Other Flatfish	0	0.0940	0	0.0018	0.0036	0
Dragonets	0	0	0	0.0180	0.0057	0.0015
Mackerel	0	0	0	0.0060	0.0206	0.0008
Ling	0	0	0	0	0	0
Other Demersals	0	0.2480	0	0.0640	0.0243	0
Herring	0	0.0513	0	0.0027	0.0036	0
Other Planktivorous Fish	0	0.1026	0	0.0053	0.0072	0
Sandeels	0	0.1340	0	0.0040	0.0240	0.0090
Epifaunal Macrobenthos	0.6650	0.3140	0	0.2510	0.3780	0.1206
Epifaunal Mesobenthos	0.0150	0	0	0.0310	0.0449	0.0839
Infaunal Macrobenthos	0.2000	0.0010	0	0	0	0.0129
Infaunal Mesobenthos	0	0.0010	0	0	0	0.0129
Infauna (Polychaete)	0.0350	0	0	0.0210	0.0672	0.0676
Lobster and Large Crabs	0	0.0400	0	0	0	0
Nephrops	0	0	0	0.0010	0.0280	0
Cephalopods	0.0850	0	0	0.0070	0.0023	0.0015
Prawns and Shrimp	0	0.0010	0	0.4530	0.0529	0.0482
Sessile Epifauna	0	0	0	0	0	0.0008
Meiofauna	0	0	0	0	0	0
Zooplankton	0	0.0130	1.0000	0.1080	0.2823	0.4837

(*continued*)

Prey \ predator	Large Sharks	Small Sharks	Basking Sharks	Skates and Rays	Cod	Haddock
Seaweed	0	0	0	0	0	0.0008
Microflora	0	0	0	0	0	0
Phytoplankton	0	0	0	0	0.0215	0.1484
Particulate Organic Matter	0	0	0	0.0070	0	0
Dissolved Organic Matter	0	0	0	0	0	0
Discards	0	0	0	0	0	0

Prey \ predator	Plaice	Whiting	Sole	Monkfish	Dab	Other flatfish
Bottlenose Dolphin	0	0	0	0	0	0
Harbour Porpoise	0	0	0	0	0	0
Minke Whale	0	0	0	0	0	0
Common Seal	0	0	0	0	0	0
Grey Seal	0	0	0	0	0	0
Seabirds	0	0	0	0	0	0
Large Sharks	0	0	0	0	0	0
Small Sharks	0	0	0	0	0	0
Basking Sharks	0	0	0	0	0	0
Skates and Rays	0	0	0	0	0	0
Cod	0	0.0200	0	0.0110	0.0020	0.0411
Haddock	0	0.0200	0	0.0055	0.0020	0.0411
Plaice	0.0042	0	0	0.1044	0	0
Whiting	0	0.0100	0	0.0110	0.0020	0.0002
Sole	0	0.0100	0	0.0440	0	0
Monkfish	0	0.0500	0	0	0.1000	0.0112
Dab	0	0.0219	0	0.0778	0.0015	0.0002
Other Flatfish	0	0.0581	0	0.1343	0.0025	0.0003
Dragonets	0.0056	0.0060	0	0.1055	0.0100 (0.1000)	0.0100 (0.0112)
Mackerel	0	0.0240	0	0.1363	0.0050	0.0006
Ling	0	0	0	0	0	0
Other Demersals	0.0056	0.1740	0	0.2000	0.2040 (0.2199)	0.1282
Herring	0	0.0480	0	0.0351	0.0127	0.0165
Other Planktivorous Fish	0	0.0959	0	0.0703	0.0253	0.0331
Sandeels	0.0112	0.1100	0	0.0110	0.0200	0.1064
Epifaunal Macrobenthos	0.0562	0.1160	0.1000	0.0110	0.1540	0.1110 (0.1381)
Epifaunal Mesobenthos	0.1404	0.0170	0.2500	0	0.0020	0.0095
Infaunal Macrobenthos	0.1404	0	0.2500	0	0	0.0093
Infaunal Mesobenthos	0.1050	0	0.1500	0	0	0
Infauna (Polychaete)	0.2277	0.0120	0.2500	0.0110	0.2200 (0.1140)	0.1200 (0.1336)
Lobster and Large Crabs	0	0	0	0.0077	0	0
Nephrops	0	0.0010	0	0.0033	0.0009	0.0001
Cephalopods	0	0.0160	0	0	0.0070	0.0380
Prawns and Shrimp	0.0624	0.0850	0	0.0209	0.1070	0.1235
Sessile Epifauna	0	0	0	0	0.0004	0
Meiofauna	0	0	0	0	0	0
Zooplankton	0.1997	0.1050	0	0	0.1220	0.1993
Seaweed	0	0	0	0	0	0
Microflora	0	0	0	0	0	0
Phytoplankton	0.0416	0	0	0	0	0
Particulate Organic Matter	0	0	0	0	0	0
Dissolved Organic Matter	0	0	0	0	0	0
Discards	0	0	0	0	0	0

Prey \ predator	Dragonet	Mackerel	Ling	Other Demersals	Herring	Other Planktiv-orous Fish
Bottlenose Dolphin	0	0	0	0	0	0
Harbour Porpoise	0	0	0	0	0	0
Minke Whale	0	0	0	0	0	0
Common Seal	0	0	0	0	0	0
Grey Seal	0	0	0	0	0	0
Seabirds	0	0	0	0	0	0
Large Sharks	0	0	0	0	0	0
Small Sharks	0	0	0	0	0	0
Basking Sharks	0	0	0	0	0	0
Skates and Rays	0	0.0010	0	0	0	0
Cod	0	0	0	0.0040	0	0
Haddock	0	0	0	0.0004	0	0
Plaice	0	0	0	0	0	0
Whiting	0	0	0	0.0019	0	0
Sole	0	0	0	0.0031	0	0
Monkfish	0	0	0	0	0	0
Dab	0	0	0	0.0027	0	0

(*continued on next page*)

(*continued*)

Prey \ predator	Dragonet	Mackerel	Ling	Other Demersals	Herring	Other Planktiv-orous Fish
Other Flatfish	0	0	0	0.0019	0	0
Dragonets	0	0	0	0.0098	0	0
Mackerel	0	0.0007	0	0.0098	0	0
Ling	0	0	0	0	0	0
Other Demersals	0	0.0010	0	0.0325	0.0100	0.0100
Herring	0	0.0030	0	0.0095	0.0007	0.0007
Other Planktivorous Fish	0	0.0060	0	0.0190	0.0013	0.0013
Sandeels	0	0	0	0.0085	0	0
Epifaunal Macrobenthos	0.6420	0.0280	0.5000	0.0914	0.0280	0.0280
Epifaunal Mesobenthos	0	0.0090	0	0.0781	0.0060	0.0060
Infaunal Macrobenthos	0	0	0	0.0006	0	0
Infaunal Mesobenthos	0	0	0	0.0003	0	0
Infauna (Polychaete)	0.2860	0.0007	0	0.0207	0.0020	0.0020
Lobster and Large Crabs	0	0	0	0	0	0
Nephrops	0	0	0.0500	0.0018	0	0
Cephalopods	0	0.0010	0	0.0033	0.0005	0.0005
Prawns and Shrimp	0	0	0.4500	0.1538	0.0060	0.0060
Sessile Epifauna	0	0	0	0	0	0
Meiofauna	0	0	0	0	0	0
Zooplankton	0.0720	0.9373	0	0.4772	0.9455	0.9455
Seaweed	0	0	0	0	0	0
Microflora	0	0	0	0	0	0
Phytoplankton	0	0.0003	0	0	0	0
Particulate Organic Matter	0	0.0120	0	0.0697	0	0
Dissolved Organic Matter	0	0	0	0	0	0
Discards	0	0	0	0	0	0

Prey \ predator	Sandeels	Epifaunal Macro-benthos	Epifaunal Meso-benthos	Infaunal Macro-benthos	Infaunal Meso-benthos	Infauna Polychaete
Bottlenose Dolphin	0	0	0	0	0	0
Harbour Porpoise	0	0	0	0	0	0
Minke Whale	0	0	0	0	0	0
Common Seal	0	0	0	0	0	0
Grey Seal	0	0	0	0	0	0
Seabirds	0	0	0	0	0	0
Large Sharks	0	0	0	0	0	0
Small Sharks	0	0	0	0	0	0
Basking Sharks	0	0	0	0	0	0
Skates and Rays	0	0	0	0	0	0
Cod	0	0	0	0	0	0
Haddock	0	0	0	0	0	0
Plaice	0	0	0	0	0	0
Whiting	0	0	0	0	0	0
Sole	0	0	0	0	0	0
Monkfish	0	0	0	0	0	0
Dab	0	0	0	0	0	0
Other Flatfish	0	0	0	0	0	0
Dragonets	0	0	0	0	0	0
Mackerel	0	0	0	0	0	0
Ling	0	0	0	0	0	0
Other Demersals	0	0	0	0	0	0
Herring	0	0	0	0	0	0
Other Planktivorous Fish	0	0	0	0	0	0
Sandeels	0	0	0	0	0	0
Epifaunal Macrobenthos	0	0.0270	0	0.0220	0	0
Epifaunal Mesobenthos	0	0.1040	0.0100	0.0220	0.0059	0
Infaunal Macrobenthos	0	0.1760	0	0.0120	0	0
Infaunal Mesobenthos	0	0.1770	0.3200	0.1330	0.0059	0
Infauna (Polychaete)	0	0.1780	0.3200	0.1330	0.0554	0
Lobster and Large Crabs	0	0	0	0	0	0
Nephrops	0	0	0	0	0	0
Cephalopods	0	0	0	0	0	0
Prawns and Shrimp	0	0	0	0	0	0
Sessile Epifauna	0	0.0060	0	0	0.0495	0
Meiofauna	0	0	0.3000	0.1120	0.1484	0
Zooplankton	0.6000	0.0760	0	0.1640	0.0425	0
Seaweed	0	0.0390	0.0400	0	0	0
Microflora	0	0.0370	0.0100	0.0010	0.1098	0.3300
Phytoplankton	0.1000	0.0190	0	0.2710	0.1098	0
Particulate Organic Matter	0.3000	0.1420 (0.1210)	0	0.0650	0.1650 (0.1098)	0.3400
Dissolved Organic Matter	0	0.0190	0	0.0650	0.3076	0.3300
Discards	0	0 (0.0210)	0	0	0 (0.0554)	0

Prey \ predator	Lobster and Large Crabs	Nephrops	Cephalo-pods	Prawns and Shrimp	Sessile Epifauna	Meio-fauna
Bottlenose Dolphin	0	0	0	0	0	0
Harbour Porpoise	0	0	0	0	0	0
Minke Whale	0	0	0	0	0	0
Common Seal	0	0	0	0	0	0
Grey Seal	0	0	0	0	0	0
Seabirds	0	0	0	0	0	0
Large Sharks	0	0	0	0	0	0
Small Sharks	0	0	0	0	0	0
Basking Sharks	0	0	0	0	0	0
Skates and Rays	0	0	0	0	0	0
Cod	0	0	0.0098	0	0	0
Haddock	0	0	0.0098	0	0	0
Plaice	0	0	0.0098	0	0	0
Whiting	0	0	0.0010	0	0	0
Sole	0	0	0.0098	0	0	0
Monkfish	0	0	0	0	0	0
Dab	0	0	0.0072	0	0	0
Other Flatfish	0	0	0.0026	0	0	0
Dragonets	0	0	0	0	0	0
Mackerel	0	0	0	0	0	0
Ling	0	0	0	0	0	0
Other Demersals	0	0.0090	0.0029	0	0	0
Herring	0	0	0.0003	0	0	0
Other Planktivorous Fish	0	0	0.0007	0	0	0
Sandeels	0	0	0.0010	0	0	0
Epifaunal Macrobenthos	0.0500	0.0700	0.0196	0	0	0
Epifaunal Mesobenthos	0.0500	0.0700	0.0196	0	0	0
Infaunal Macrobenthos	0.0500	0.0700	0.0196	0	0	0
Infaunal Mesobenthos	0.0500	0.0700	0.0196	0	0	0
Infauna (Polychaete)	0	0.0500	0.0098	0	0	0.0100
Lobster and Large Crabs	0.0300	0	0.0049	0	0	0
Nephrops	0	0	0.0010	0	0	0
Cephalopods	0	0	0.0010	0	0	0
Prawns and Shrimp	0.1700 (0.1500)	0	0.0098	0	0	0
Sessile Epifauna	0	0.1610	0	0	0	0
Meiofauna	0	0	0	0	0	0.0900
Zooplankton	0	0	0.6438	0.0900	0.2970	0
Seaweed	0	0	0	0	0	0
Microflora	0	0	0	0	0.1430	0.7000
Phytoplankton	0	0	0.1963	0.0800	0.1430	0
Particulate Organic Matter	0.6000 (0.6200)	0.4700 (0)	0	0.5200	0.1430	0.2000
Dissolved Organic Matter	0	0	0	0.3100	0.2740	0
Discards	0.0200 0	0.0300 (0.5000)	0	0	0	0

References

Ames, D.P., Horsburgh, J.S., Cao, Y., Kadlec, J., Whiteaker, T., Valentine, D., 2012. HydroDesktop: web services-based software for hydrologic data discovery, download, visualization, and analysis. Environ. Model. Software 37, 146–156. https://doi.org/10.1016/J.ENVSOFT.2012.03.013.

Begg, F., Coop, G., Baxter, M., Scott, E., McCartney, M., 1992. Anthropogenic radiocarbon in the eastern Irish Sea and Scottish coastal waters. Radiocarbon 34, 707–716.

Booth, S., Zeller, D., 2005. Mercury, food webs, and marine mammals: implications of diet and climate change for human health. Environ. Health Perspect. 113, 521–526. https://doi.org/10.1289/ehp.7603.

Chester, R., 1990. Marine Geochemistry. Unwin Hyman, London.

Christensen, V., Walters, C.J., 2004. Ecopath with Ecosim: methods, capabilities and limitations. Ecol. Modell 172, 109–139. https://doi.org/10.1016/j.ecolmodel.2003.09.003.

Colleter, M., Valls, A., Guitton, J., Gascuel, D., Pauly, D., Christensen, V., 2015. Global overview of the applications of the Ecopath with Ecosim modeling approach using the EcoBase models repository. Ecol. Modell 302, 42–53. https://doi.org/10.1016/j.ecolmodel.2015.01.025.

Cook, G.T., Begg, F.H., Naysmith, P., Scott, E.M., McCartney, M., 1995. Anthropogenic ^{14}C marine geochemistry in the vicinity of a nuclear fuel reprocessing plant. Radiocarbon 37, 459–467.

Cook, G., MacKenzie, A., Muir, G., Mackie, G.,P.,G., 2004. Sellafield-derived anthropogenic C-14 in the marine intertidal environment of the NE Irish Sea. Radiocarbon 46, 877–883.

Cook, G., MacKenzie, A., Naysmith, P., Anderson, R., 1998. Natural and anthropogenic ^{14}C in the UK coastal marine environment. J. Environ. Radioact. 40, 89–111.

Crozier, W.W., 1985. Observations on the food and feeding of the angler-fish, Lophius piscatorius, in the Northern Irish Sea. Fish. Soc. Br. Isles 655–665. https://doi.org/10.1111/j.1095-8649.1985.tb03210.x.

Dabrowski, T., Hartnett, M., 2008. Modelling travel and residence times in the eastern Irish Sea. Mar. Pollut. Bull. 57, 41–46. https://doi.org/10.1016/j.marpolbul.2008.03.014.

Dabrowski, T., Hartnett, M., Olbert, A.I., 2010. Influence of seasonal circulation on flushing of the Irish Sea. Mar. Pollut. Bull. 60, 748–758. https://doi.org/10.1016/j.marpolbul.2009.11.018.

Ellis, J.R., Pawson, M.G., Shackley, S.E., 1996. The comparative feeding ecology of six species of shark and four species of ray (Elasmobranchii) in the North-East Atlantic. J. Mar. Biol. Assoc. U. K. 76, 89. https://doi.org/10.1017/S0025315400029039.

Froese, R., Pauly, D., 2016. FishBase. World Wide Web electronic publication. www.fishbase.org (accessed 08.2016).

Gibson, R.N., Ezzi, I.A., 1987. Feeding relationships of a demersal fish assemblage on the west coast of Scotland. J. Fish. Biol. 31, 55–69. https://doi.org/10.1111/j.1095-8649.1987.tb05214.x.

Gowen, R.J., Bloomfield, S.P., 1996. Chlorophyll standing crop and phytoplankton production in the western Irish Sea during 1992 and 1993. J. Plankton Res. 18, 1753–1751.

Gowen, R.J., Mills, D.K., Trimmer, M., Nedwell, D.B., 2000. Production and its fate in two coastal regions of the Irish Sea: the influence of anthropogenic nutrients. Mar. Ecol. Prog. Ser. 208, 51–64. https://doi.org/10.3354/meps208051.

Gulliver, P., Cook, G., MacKenzie, A., Naysmith, P., Anderson, R., 2001. Transport of sellafield-derived C-14 from the Irish sea through the north channel. Radiocarbon 43, 869–877.

Gulliver, P., Cook, G., MacKenzie, A., Naysmith, P., Anderson, R., 2004. Sources of anthropogenic C-14 to the north sea. Radiocarbon 46, 869–875.

Hernandez-Milian, G., 2014. Trophic Role of Small Cetaceans and Seals in Irish Waters. PhD Thesis. University College Cork, Ireland.

Heymans, J.J., Coll, M., Link, J.S., Mackinson, S., Steenbeek, J., Walters, C.,

Christensen, V., 2016. Best practice in Ecopath with Ecosim food-web models for ecosystem-based management. Ecol. Modell 331, 173–184. https://doi.org/10.1016/j.ecolmodel.2015.12.007.

Hughes, D.J., Ansell, A.D., Atkinson, R.J.A., 1996. Sediment bioturbation by the echiuran worm Maxmuelleria lankesteri (Herdman) and its consequences for radionuclide dispersal in Irish Sea sediments. J. Exp. Mar. Biol. Ecol. 195, 203–220.

Jefferies, D., Preston, A., Steele, A., 1973. Distribution of caesium-137 in British coastal waters. Mar. Pollut. Bull. 4, 118–122.

Kahle, D., Wickham, H., 2013. Ggmap: Spatial Visualization with Ggplot2. R J. 5, pp. 144–161. https://doi.org/10.1023/A:1009843930701.

Kershaw, P.J., Swift, D.J., Pentreath, R.J., Lovett, M.B., 1983. Plutonium redistribution in Irish Sea sediments by biological activity. Nature 306, 774–775.

Kershaw, P.J., Swift, D.J., Pentreath, R.J., Lovett, M.B., 1984. The incorporation of plutonium, americium and curium into the Irish Sea seabed by biological activity. Sci. Total Environ. 40, 61–81.

Kershaw, P.J., Denoon, D.C., Woodhead, D.S., 1999. Observations on the redistribution of plutonium and americium in the Irish Sea sediments, 1978 to 1996: concentrations and inventories. J. Environ. Radioact. 44, 191–221.

Kershaw, P.J., Baxter, A., 1995. The transfer of reprocessing wastes from north-west Europe to the Arctic. Deep Sea Res. Part II Top. Stud 42, 1413–1448.

Kershaw, P.J., Heldal, H.E., Mork, K.A., Rudjord, A.L., 2004. Variability in the supply, distribution and transport of the transient tracer ^{99}Tc in the NE Atlantic. J. Mar. Syst. 44, 55–81. https://doi.org/10.1016/j.jmarsys.2003.08.003.

Larsen, L.-H., Sagerup, K., Ramsvatn, S., 2016. The mussel path – using the contaminant tracer, Ecotracer, in Ecopath to model the spread of pollutants in an Arctic marine food web. Ecol. Modell 331, 77–85. https://doi.org/10.1016/j.ecolmodel.2015.10.011.

Lees, K., Mackinson, S., 2007. An Ecopath model of the Irish Sea : ecosystems properties and sensitivity. Sci. Ser. Tech Rep., Cefas Lowestoft 138, 49.

Link, J.S., 2010. Adding rigor to ecological network models by evaluating a set of pre-balance diagnostics: a plea for PREBAL. Ecol. Modell 221, 1580–1591. https://doi.org/10.1016/j.ecolmodel.2010.03.012.

MacKenzie, A.B., Cook, G.T., Barth, J., Gulliver, P., McDonald, P., 2004. ^{14}C and δ^{13}C characteristics of organic matter and carbonate in saltmarsh sediments from south west Scotland. J. Environ. Monit. 6, 441–447. https://doi.org/10.1039/b315766k.

McGill, L.M., Gerig, B.S., Chaloner, D.T., Lamberti, G.A., 2017. An ecosystem model for evaluating the effects of introduced Pacific salmon on contaminant burdens of stream-resident fish. Ecol. Modell 355, 39–48. https://doi.org/10.1016/j.ecolmodel.2017.03.027.

Muir, G.K.P., Cook, G.T., Tripney, B.G., Mackenzie, A.B., Stewart, H., Tierney, K.M., 2015. Temporal trend in the transfer of Sellafield-derived ^{14}C into different size fractions of the carbonate component of NE Irish Sea sediment. Radiocarbon 57 (3), 347–354.

Muir, G.K.P., Tierney, K.M., Cook, G.T., MacKinnon, G., Howe, J.A., Heymans, J.J., Hughes, D.J., Xu, S., 2017. Ecosystem uptake and transfer of Sellafield-derived radiocarbon (^{14}C). Part 1. The Irish Sea. Mar. Pollut. Bull. 114, 792–804. https://doi.org/10.1016/j.marpolbul.2016.10.072.

Niiranen, S., Stipa, T., Hirvonen, A., Paakkonen, J.P., Norkko, A., 2008. Modelled bioaccumulation of chemical warfare agents within the baltic sea food web. US/EU-Baltic Int. Symp. Ocean Obs. Ecosyst. ManagForecast. - Provisional Symp. Proceedings, Balt. https://doi.org/10.1109/BALTIC.2008.4625532.

Nuclear Decommissioning Authority, 2016. Monitoring Our Environment Discharges and Environmental Monitoring Annual Report. Sellafield Ltd.

Polovina, J.J., 1984. Coral reefs model of a coral reef ecosystem. Coral Reefs 3, 1–11. https://doi.org/10.1007/bf00306135.

R Development Core Team, 2016. R: a Language and Environment for Statistical Computing. R Foundation for Statistical Computing, Vienna, Austria. http://www.R-project.org.

Sandberg, J., Kumblad, L., Kautsky, U., 2007. Can ECOPATH with ECOSIM enhance models of radionuclide flows in food webs? - an example for ^{14}C in a coastal food web in the Baltic Sea. J. Environ. Radioact. 92, 96–111. https://doi.org/10.1016/j.jenvrad.2006.09.010.

Sanderson, H., Fauser, P., Thomsen, M., Vanninen, P., Soderstrom, M., Savin, Y., Khalikov, I., Hirvonen, A., Niiranen, S., Missiaen, T., Gress, A., Borodin, P., Medvedeva, N., Polyak, Y., Paka, V., Zhurbas, V., Feller, P., 2010. Environmental hazards of sea-dumped chemical weapons. Environ. Sci. Technol. 44, 4389–4394. https://doi.org/10.1021/es903472a.

Steenbeek, J., Coll, M., Gurney, L., Mélin, F., Hoepffner, N., Buszowski, J., Christensen, V., 2013. Bridging the gap between ecosystem modeling tools and geographic information systems: driving a food web model with external spatial–temporal data. Ecol. Modell 263, 139–151. https://doi.org/10.1016/j.ecolmodel.2013.04.027.

Tierney, K.M., Muir, G.K.P., Cook, G.T., MacKenzie, A.B., MacKinnon, G., Heymans, J.J., Xu, S., Howe, J.A., 2016. Accumulation of sellafield-derived ^{14}C in Irish sea and west of Scotland intertidal shells and sediments. J. Environ. Radioact. 151, 321–327. https://doi.org/10.1016/j.jenvrad.2015.10.029.

Tierney, K.M., Muir, G.K.P., Cook, G.T., MacKinnon, G., Howe, J.A., Heymans, J.J., Hughes, D.J., Xu, S., 2017a. Ecosystem uptake and transfer of Sellafield-derived radiocarbon (^{14}C) part 2: the West of Scotland. Mar. Pollut. Bull. 115, 57–66. https://doi.org/10.1016/j.marpolbul.2016.11.014.

Tierney, K.M., Muir, G.K.P., Cook, G.T., Heymans, J.J., MacKinnon, G., Howe, J.A., Xu, S., Brownlow, A., Davison, N.J., ten Doeschate, M., Deaville, R., 2017b. Nuclear reprocessing-related radiocarbon (^{14}C) Uptake into UK Marine Mammals. Mar. Pollut. Bull. Accepted.

Walters, C., Christensen, V., Pauly, D., 1997. Structuring dynamic models of exploited ecosystems from trophic mass-balance assessments. Rev. Fish Biol. Fish. 7, 139–172. https://doi.org/10.1023/A:1018479526149.

Walters, C., Pauly, D., Christensen, V., 1999. Prediction of mesoscale patterns in trophic spatial of exploited relationships the ecosystems, with emphasis on impacts of marine protected areas. Ecosystems 2, 539–554.

Walters, W.J., Christensen, V., 2017. Ecotracer: analyzing concentration of contaminants and radioisotopes in an aquatic spatial-dynamic food web model. J. Environ. Radioact. 181, 118–127. https://doi.org/10.1016/j.jenvrad.2017.11.008.